AN ABSTRACT OF THE THESIS OF

George R. Tuttle for the degree of Master of Science in Toxicology presentation on October 30, 2012.
TITLE: Size and Surface Area Dependent Toxicity of Silver Nanoparticles in Zebrafish Embryos (*Danio rerio*)

Abstract approved:

Stacey L. Harper

Many studies addressing the toxicity of silver nanomaterials have found that smaller sized silver nanoparticles are usually more toxic to organisms and in cell culture than particles of larger sizes yet it is not entirely clear why. We investigated the size dependent toxicity of silver nanoparticles by measuring the response of embryonic zebrafish (*Danio rerio*) following exposure to a library of thirteen distinct silver nanoparticle size distributions with mean diameters between 8.9 nm and 112.6 nm. Data analysis using dose-response modeling revealed that silver nanoparticles (AgNP) induced embryo toxicity that is dependent on the total surface area and not on the mass or particle number in solution. Included in this study is a comparison between embryo toxicity induced by silver nitrate ($AgNO_3$) and AgNPs for cardiovascular endpoints, as well as an investigation into the influence of the chorion on AgNP toxicity. This study demonstrates the importance of using alternative dose metrics in nanotoxicology, and highlights the value of using the embryonic zebrafish to explore nanomaterial structure activity relationships.

Size and Surface Area Dependent Toxicity of Silver Nanoparticles in Zebrafish Embryos (*Danio rerio*)

by

George R. Tuttle

A THESIS

Submitted to

Oregon State University

in partial fulfillment of
the requirement for the
degree of

Master of Science

Presented October 30, 2012
Commencement June 2013

Master of Science thesis of George R. Tuttle presentation on October 30 2012.

APPROVED:

Major Professor, Representing Toxicology

Head of the Department of Environmental and Molecular Toxicology

---

Dean of the Graduate School

I understand that my thesis will become part of the permanent collection of the Oregon State University Libraries. My signature below authorizes release of my thesis to any reader upon request.

George R. Tuttle, Author

ACKNOWLEGMENTS

The author expresses heartfelt appreciation to his mentor and advisor Dr. Stacey L. Harper, his committee members, research group, collaborators, friends and loving family for all of their amazing support and encouragement.

TABLE OF CONTENTS

TABLE OF CONTENTS (Continued)

LIST OF FIGURES

Figure Page

LIST OF FIGURES (Continued)

Figure Page

LIST OF TABLES

Tables Page

Size and Surface Area Dependent Toxicity of Silver Nanoparticles in Zebrafish Embryos (*Danio rerio*)

Chapter 1: Introduction

1.1 Nanosilver Background

Silver, in its various inorganic forms, has been in use long before the advent of engineered nanomaterials (ENMs). Silver nanomaterials (nanosilver) have become one of the leading nanomaterials used to create nanoenabled consumer products. Silver nanoparticles (AgNPs) are characteristically spherical in shape and represent one form of nanosilver. While AgNPs have several potential applications due to their unique optical properties, the primary application for AgNPs exploits their potent anti-microbial properties (Chen and Schluesener, 2008; Hwang et al., 2008; Liu et al., 2010; Sotiriou et al., 2011; Rai et al., 2012). Nanosilver has been incorporated into consumer goods including textiles, contraceptives, cosmetics, children's toys, medical equipment, air filters, water filters, and residential washing machines (Stensberg et al., 2011). Because of the growing utilization of nanosilver in common consumer products, and the growing interest in nanosilver applications, concerns are being raised over the unforeseen and potentially adverse effects that these materials could pose to humans and environment (Benn et al., 2010). Benn et al., (2010) found that nanosilver had been incorporated into several consumer products including an athletic shirt, a medical mask, medical cloth, toothpaste, shampoo, detergent, a towel, a toy teddy bear and two humidifiers at concentrations ranging from 1.4 μg/g to 270 mg/g. Benn et al., (2010) also found that these products leached up to 45 μg of silver per gram of product when washed with tap water. Although the anti-microbial properties of nanosilver are typically attributed to the release of Ag+ ions as a result of particle dissolution, research suggests that nanomaterials may elicit toxicity that is not fully attributed to the release of Ag+ ions.

1.2 Literature Review:

1.2.1 *In vitro* AgNP Toxicity

The toxicity of nanosilver to living systems has been investigated extensively using both *in vitro* and *in vivo* systems. Numerous results from *in vitro* studies report that silver nanomaterials induced cytotoxicity and reactive oxygen species (ROS) generation (Carlson et al., 2008; AshaRani et al., 2009; Park et al., 2011a; b; Piao et al., 2011). Carlson et al., (2008) showed a significant dose-dependent and size-dependent decrease in mitochondrial function (MTT assay), mitochondrial membrane integrity (LDH assay), ROS generation (DCFH-DA assay), release of inflammatory cytokines (TNF-α, MIP-2, and IL-1β) and

glutathione depletion in rat alveolar macrophages. AshaRani et al., (2009) reported increased ROS generation and excess oxidative stress, resulting from the intercellular production of hydrogen peroxide and superoxide in AgNP treated cells. AshaRani et al., (2009) also showed decreased metabolic activity associated with a reduction in ATP production in treated cells, suggesting mitochondrial dysfunction. The *in vitro* findings demonstrated that exposure to AgNPs can result in genotoxicity from increased oxidative stress (AshaRani et al., 2009; Park et al., 2011b; Piao et al., 2011). Starch stabilized AgNPs induced DNA damage, increased chromosomal aberrations, and caused G_2/M cell cycle arrest in cancerous and non-cancerous human cell lines (AshaRani et al., 2009). Several studies used electron microscopy to show translocation of AgNPs into cellular compartments including the cytosol, nucleus, mitochondria, and endosomes (AshaRani et al., 2009; Carlson et al., 2008). Although the results of these investigations allude to the nature of the mechanisms involved in AgNP mediated toxicity, the exact mechanisms remain elusive and important questions regarding the way in which specific nanomaterial properties play a role in modulating toxicity remain unanswered.

1.2.2 Size Dependent *In vitro* Toxicity

Many *in vitro* studies describing AgNP toxicity have provided evidence for the relationship between particle size and the degree of toxicity (Carlson et al., 2008; Park et al., 2011a; b). Particle size has been implicated as an important physical characteristic of nanomaterials that is often predictive of toxicity (Oberdörster et al., 2005; Nel, 2006; Nel et al., 2012). Many nanomaterial properties vary as a function of particle size including particle mass, volume, surface area, particle number, and the percentage of atoms at the particle surface. Toxicity could potentially be a function of particle size due to its relationship to dissolution rate, amount of reactive surface area, or bioavailability. Primary physical characteristics, such as shape, surface area, surface chemistry, chemical composition, surface charge, and crystallinity may influence particle toxicity (Nel et al., 2012). Many secondary characteristics including particle solubility, polydispersity, agglomerate size, aggregate size, rate of dissolution, hydrophobicity, etc. may also contribute to particle toxicity. Understanding how differences in nanomaterial characteristics lead to changes in toxicity is an important aspect of nanotoxicology and one that requires the use of alternative dose metrics.

1.2.3 AgNP Oxidative Dissolution

Dissolution describes the decomposition of metal oxide and zero valent metal nanomaterial species (ex: Ag^0) into their constituent metal ions. Studies designed to investigate the environmental fate, transformation and stability of silver nanomaterials show that silver nanomaterials undergo oxidative dissolution in systems where oxygen and protons are present, resulting in the release of silver Ag^+ ions in solution over time (Zhang et al., 2011; Kittler et al., 2010; Liu and Hurt, 2010; Ma et al., 2012; Lok et al., 2007). Liu and Hurt, (2010) showed that dissolved oxygen and protons are necessary for dissolution to occur. Liu and Hurt, (2010) also showed that the rate of oxidative dissolution of AgNPs increases with increasing temperature, time, and concentration, but decreases with increasing pH, salinity, and following addition of natural organic matter (humic or fulvic acids). Several studies clearly demonstrate that the oxidative dissolution of AgNPs is strongly dependent on particle size, where smaller particle sizes release more silver ions due to their greater surface area to mass ratio (Zhang et al., 2011; Ma et al., 2012).

1.2.4 Silver Ion Mediated Toxicity

A central question regarding AgNP toxicity is whether the observed toxicity is mediated solely by ionic silver released by the oxidative dissolution of nanosilver or if there are mechanisms of toxicity inherent to the NP itself. The toxicity of many ENMs are associated with the release of metal ions, and that higher rates of dissolution are often associated with increased toxicity (Lok et al., 2007; Kittler et al., 2010). Lok et al., (2007) specifically showed that surface oxidation of AgNPs is necessary to produce antibacterial activity and that particle size can determine the rate of particle dissolution. Furthermore, the oxidative dissolution of AgNP produces hydrogen peroxide and depletes both dissolved oxygen and protons (Liu and Hurt, 2010), which could contribute to the intercellular ROS generation. Although Ag^+ ions contribute significantly to the toxicity of AgNPs, it is difficult to know for certain whether the toxicity associated with nanomaterials is due solely to the release of metal ions or if an alternative mechanism of AgNP toxicity exists. The potential that AgNPs may be associated with some alternative mechanism of toxicity brings into question concerns regarding human health and whether AgNPs can be regulated under the same guidelines as other forms of silver. Determining if alternative mechanisms exist and which physicochemical properties result in increased or decreased toxicity are necessary steps in assessing the potential risks posed by these novel materials.

1.2.5 *In vivo* AgNP Toxicity

Silver is acutely toxic to many forms of aquatic and terrestrial life and the toxicity of AgNPs often exceeds that of other metal and metal oxide nanoparticles, including Au, Pt, SiO_2, Al_2O_3, CuO, NiO, ZnO, Co_3O_4, Ni and TiO_2 (George et al., 2011; Lin et al., 2011; Griffitt et al., 2008b). Findings from a diverse array of *in vivo* animal models including *Caenorhabditis elelgans* (Roh et al., 2009; Meyer et al., 2010; Yang et al., 2012), *Drosophila melanogaster* (Ahamed et al., 2010; Webster et al., 2011), *Daphnia magna* (Stensberg et al., 2011; Römer et al., 2011; Lee et al., 2012; Georgantzopoulou et al., 2012), *Chlamydomonas rinehardii* (Navarro et al., 2008), and several teleosts models (Shaw and Handy, 2011) show that both Ag+ ions and AgNPs are acutely toxic and elicit a variety of sub-lethal responses, including physiological, neurological, behavioral and biochemical endpoints.

1.2.6 Embryonic Zebrafish (*Danio rerio*)

One animal model being used extensively to address the toxicity of AgNPs and other ENMs is the zebrafish (*Danio rerio*). Zebrafish are rapidly gaining a reputation as an important animal model for conducting nanomaterials hazard assessments. Zebrafish embryos are ideal for this application because of their small size, high reproductive capacity, short developmental period, and ease of culture. Because of these qualities, embryonic zebrafish are particularly valuable for conducting medium to high throughput studies and systematic toxicity evaluations across multiple materials which can then be used to generate structural activity relationships (Harper et al., 2008b; a, 2011; George et al., 2011; Lin et al., 2011; Bar-Ilan et al., 2009).

1.2.7 AgNP and Ag^+ Mediated Toxicity in Zebrafish

Embryonic zebrafish have been used in many studies to investigate the toxicity of AgNPs (Lee et al., 2007; Asharani et al., 2008; Yeo and Kang, 2008; Min-Kyeong Yeo and Jae-Won Yoon, 2009; Bar-Ilan et al., 2009; Powers et al., 2010; George et al., 2012; Bowman et al., 2012). Of these previous studies, many report similar observations regarding the type and magnitude of the response. Specifically, Asharani et al., (2008) found that starch and BSA stabilized AgNPs caused dose dependent embryo mortality, severe dismorphology (bent spine and cloudy appearance of chorionic fluid), cardiovascular defects, including pericardial edema, and depressed heart rate as well as decreased hatching rate. Bar-Ilan et

al., (2009) confirmed the dose dependent effects reported by Asharani et al., (2008) and also demonstrated size dependent effects in which smaller AgNP were more toxic than larger particles. George et al., (2011 and 2012) reported similar morpholigical malformations (bent axis, opaque yolk, and stunted growth), pericardial edema, heart rate depression, and reduced hatch rate following exposure to polyvinylpyrrolidone (PVP) stabilized AgNPs.

1.2.8 AgNP Mediated Toxicity in Adult and Larval Zebrafish

In adult zebrafish treated with AgNPs, Choi et al., (2010) observed heightened oxidative stress response, induced apoptosis, increased glutathione levels, increased lipid peroxidation, and translocation of AgNP in to the cytosol and nuclear membrane. Increased levels of γ-H2AX, a marker of double stranded DNA breaks, and p53, an important tumor suppressor protein, were observed in AgNP treated zebrafish as well as increased expression of p53 target genes (*Bax, Noxa,* and *p21*) in the liver of adult fish indicating DNA damage (Choi et al., 2010). Unfortunately, in the study by Choi et al. (2010), no fish were treated with $AgNO_3$ and therefore gene expression changes were not directly compared between AgNPs and a direct source of soluble Ag^+ ions. Another study found that, adult zebrafish exposed to low concentrations of AgNPs had significantly higher tissue burden levels in gill tissue than in other treatments including $AgNO_3$, the dissolved silver ion fraction from AgNP suspensions, copper nanoparticles or dissolved copper ions. AgNPs did not, however, produce significant gill thickening as was observed with dissolved silver and copper ions (Griffitt et al., 2008a). Powers et al., (2010) discovered that $AgNO_3$ affects neurobehavioral endpoints in larval zebrafish, such as swimming performance and distance at sub-lethal concentrations that did not elicit changes in morphology. Differences in neurobehavioral effects for exposure to Ag^+ ions, 10 nm citrate stabilized AgNPs, 10 nm PVP stabilized AgNPs, and 50 nm PVP stabilized AgNPs were later described by Powers et al. (2011) using a visual acuity test. The study demonstrated that fish movement was altered in treated fish following alternating light and dark periods at concentrations that did not elicit malformations (Powers et al., 2011).

1.2.9 Primary Mechanism of AgNP Toxicity

Of the studies that suggest release of Ag^+ ions as the sole source of toxicity elicited from AgNP exposures, most have focused on the correlation between the concentration of

Ag+ in solution and toxicity endpoints. Choi et al. (2010) show that removal of the ions through purification of the particles reduces or even eliminates the toxicity of the particles. Other studies have shown that using ligands that bind free ionic silver also reduces AgNP toxicity (George et al., 2012). Bar-Ilan et al. (2009) showed that although both silver and gold nanoparticles are taken up by zebrafish embryos, only silver induced toxicity leading the authors to suggest a mechanism of *in vivo* particle destabilization resulting in the release of silver ions. Furthermore, Bar-Ilan and colleagues (2009) noted that malformations induced by exposure to $AgNO_3$ in their study were very similar to that those induced by AgNPs. It is important to highlight that other studies testing the effects of both AgNPs and $AgNO_3$ (Min-Kyeong Yeo and Jae-Won Yoon, 2009) also tend to show a similar spectrum and frequency of malformations indicating a similar mode of toxicity. Further evidence from Choi et al., (2010) showed that removal of silver ions from exposure solution using ion exchange resin resulted in a dose response expression of metallothionein 2 (*mt2*) induction in zebrafish liver tissue suggesting the release of free silver *in vivo*.

1.2.10 Alternative Mechanisms of Mediated Embryo Toxicity

The majority of studies show that AgNP toxicity is overwhelmingly driven by generation of Ag^+ ions through particles dissolution (Lok et al., 2007). The controversy surrounding AgNP toxicity results from a body of literature that suggests the toxicity induced by exposure to AgNPs is not fully explained by the dissolution of AgNPs, and that some particle-mediated mechanism is likely to exist (Griffitt et al., 2008a, Griffitt, et al., 2008b; Asharani et al., 2008; George et al., 2012). As an example, a particle-mediated mechanism referred to as the Trojan-horse mechanism could allow nanoparticles to gain access to cell interiors, ether forcibly by disrupting cell surfaces, or through preferential uptake by receptors or endocytosis where they could subsequently release toxic ions or react with cell interiors where metal ions or bulk metals would otherwise be excluded (Park et al., 2010). Some studies have directly compared AgNP toxicity with toxicity from $AgNO_3$ and have come to similar conclusions (Asharani et al., 2008). Griffitt, et al., (2008) found that the amount of soluble metal leached from nano-silver and nano-copper in moderately hard water over a 48h exposure period was below the no effect level for the corresponding soluble form of the metal, yet AgNPs were associated with significant toxicity to ~24hpf-48hpf juvenile zebrafish. Perhaps the most convincing evidence suggestive of a separate mechanism independent of the toxicity induced by free Ag^+ ions, was a recent publication by

George et al. (2012). This work demonstrated that nano-silver plates induced toxicity and increased ROS generation in embryonic zebrafish that were associated with defects on the plate surface (George et al., 2012). The authors suggested that a more thorough and systematic investigation of AgNP structure activity relationships is warranted and necessary to determine the properties of AgNPs that contribute to the particle-mediated toxicity of AgNPs (George et al., 2012).

1.2.11 Zebrafish Embryo Chorions Play a Role in ENM Toxicity

Many studies utilizing embryonic zebrafish remove the chorion using a protease enzyme or manual removal (Truong et al., 2011). Zebrafish chorions have numerous pores ranging in size between 0.5 and 0.7μm (Rawson et al., 2000; Lee et al., 2007). Because the chorion is thought to serve as a natural protective barrier to particulates and some chemicals, removal of the chorion may allow for greater exposure and will eliminate the chorion as a possible confounding factor. Some studies have shown that the chorions may actually increase nanoparticle toxicity. Lin et al., (2011) investigated the physiological ability of the chorion to concentrate metals in the perivitelline fluid using metal-sensitive dyes and ICP-MS, and showed that metal ions from CuO, ZnO, NiO, and Co_3O_4 metal oxide nanoparticles concentrate within the chorion. King Heiden et al. evaluated the effect of the chorion during exposures with polyamidoamine (PAMAM) dendrimers and observed greater toxicity in embryos possessing an intact chorion in comparison to those that had their chorion removed prior to exposure (King Heiden et al., 2007).

1.2.13 Size Dependent Embryo Toxicity of AgNPs

This size-dependent toxicity of AgNPs with respect to zebrafish embryos holds true for many studies that utilize multiple sizes of AgNPs (Bar-Ilan et al., 2009; George et al., 2012). Bar-Ilan et al., (2009) compared the median lethal concentration (LC_{50}) profiles from 3 nm, 10 nm, 50 nm, and 100 nm colloidal silver nanoparticles, and observed clear size-dependent and dose-dependent responses from zebrafish embryos. Bar-Ilan et al., (2009) also showed evidence for a time-dependent response using a single high concentration (250 μM), causing significantly different size dependent mortality at 24hpf which became less significant later during the exposure. This could indicate that the rate of dissolution of smaller particles caused higher mortality sooner than larger particles. Based on the available literature and on our initial observations of AgNP toxicity, AgNP embryo toxicity is

dependent upon the primary particle diameter (Bar-Ilan et al., 2009). Although AgNP toxicity seems to be size dependent, this does not specifically explain why they exhibit size dependent toxicity. In this study we investigate why AgNP toxicity is size dependent by looking at three physical parameters that all scale with particle size; mass, particle number, and surface area to determine the physical parameter that explains the phenomenon.

1.3 Study Design

1.3.1 Similarities Between $AgNO_3$ and AgNP Toxicity

In the present study, exposure to $AgNO_3$ was investigated as a direct source of soluble silver ions. We compared the similarities and differences in toxicity resulting from exposure to $AgNO_3$ with an indirect source of ions from AgNPs to determine if the source of silver ions affected the magnitude and presentation of the toxicity endpoints and whether differences might suggest an alternative mechanism for the particles.

1.3.2 Estimating the Effect of the Chorion

This study also investigated the influence of the chorion on AgNP toxicity. Limited research has been performed to directly compare nanomaterial toxicity in embryos with or without a chorion, yet it is possible that the chorion may be a confounding factor concerning ENM toxicity. To accomplish this, the effect of the presence (Ch (+)) or absence (Ch (-)) of the chorion was examined following exposure to $AgNO_3$, 10 nm AgNPs, or 100 nm AgNPs. We assessed mortality as well as two cardiovascular endpoints found to be sensitive during range finding experiments: decreased embryo heart rate at 48hpf as a measurement of a physiological response, and the frequency of pericardial edema (PE) in embryos surviving at 120hpf. The embryo toxicity between the three materials with Ch(+) or Ch(-) embryos were analyzed using three alternative dose metrics: mass concentration, particle concentration, surface area concentration.

1.3.3 Dose Modeling and Alternative Dose Metrics Analysis

The overarching aim of this study was to address the reason that size-dependence is observed in other AgNP toxicity studies. This aim was accomplished by constructing a structure activity relationship (SAR) using size-dependent, and concentration-dependent embryonic lethality following exposure to thirteen discrete AgNP size distributions, with mean primary particle diameters ranging from 8.9 nm to 112.6 nm. The results from these experiments were analyzed to determine how embryo mortality is affected in a size-

dependent manner and which particle properties that scale with primary particle diameter may be the most relevant in predicting toxicity. Embryo mortality was modeled for each particle size to estimate LC_{50} values for three different measures of concentration: the mass of the particles in solution (mass concentration), the total number of particles in solution (particle concentration), and the total surface area of the particles in solution (surface area concentration). Our hypothesis was that particle surface area that scales geometrically with particle diameter is the ultimate driver of AgNP toxicity. We show support for this hypothesis by analyzing study results and directly comparing alternative dose metrics.

Chapter 2: Materials and Methods

2.1 Test Materials

Citrate stabilized 1.0 mg/mL BioPure™ silver nanoparticles purchased from NanoComposix, Inc. (San Diego, CA) in 10 mL volumes were used through out the study with mean (± 1SD) primary particle diameters of 8.9±1.3 nm and 99.4±7 nm. Eleven other AgNP suspensions BioPure™ Silver nanoparticles were also purchased from NanoComposix, Inc. in 1 mL volumes. These samples consisted of one citrate stabilized AgNP suspension, with a mean primary particle diameter 10.2±1.7 nm, and ten phosphate stabilized AgNP suspensions with mean primary particle diameters of 20.3±1.9 nm, 34.4±3.4 nm, 41.9±3.6 nm, 53.1±4.1 nm, 61.2±5.3 nm, 67.3±5.4 nm, 79.8±5.1 nm, 90.8±7.3 nm, 102.3±9.4 nm, and 112.6±7.8 nm. $AgNO_3$ ACS, 99.9% was purchased from Alfa Aesar (Ward Hill, MA).

2.2 Nanomaterial Characterization

AgNP characteristics for each material are listed in Table 1. The manufacturer provided mean primary particle diameter and primary particle size distributions measured using a JEOL 1010 Transmission Electron Microscope (TEM) Table 1. All particle suspensions were associated with narrow size distributions and were reported as the coefficient of variation (CV). Mass concentration (g/mL) provided by the manufacturer was measured using a Thermo Fisher X Series 2 ICP-MS. Mean primary particle surface area (nm^2/particle) and mean primary particle volume (nm^3/particle(s)) were calculated using the geometric equations for surface area, $4*\pi*1/2d^2$ where d is the mean primary particle diameter measured by TEM, and $[4/3]*\pi*r^3$ is the volume of a uniform sphere with radius (r) which is half the mean primary particle diameter measured by TEM. Theoretical particle concentration (particle(s)/mL) was calculated by multiplying the mass concentration (g/mL) by the density of silver (0.001 g/cm^3) to find the volume of silver per mL (cm^3/mL). The volume of silver per mL (cm^3/mL) was then divided by mean primary particle volume (nm^3/particle) to determine the theoretical particle concentration (particles/mL). Theoretical surface area concentration (mm^2/mL) was calculated by first dividing the mean primary particle surface area (nm^2/particle(s)) by $1*10^{12}$ with appropriate units. Mean primary particle surface area (mm^2/particle(s)) was then multiplied by the theoretical particle concentration (particle(s)/mL) to yield theoretical surface area

concentration (mm^2/mL). These calculations are in accordance with previous studies (Bar-Ilan et al., 2009; George et al., 2012; Bowman et al., 2012) that utilize the TEM derived diameter to determine theoretical particle concentration and theoretical surface area concentration.

Table 1. Measured and calculated AgNPs characteristics. This table displays the (a) measurements provided by the manufacturer and (b) the particle characteristics calculated as outlined in the methods and materials section for each material used in this study. The values that refer to concentration are referring to the stock solutions from which individual treatment levels were made in equal proportions.

Mean Primary Particle Diameter [a] (nm)	Primary Particle Diameter Coefficient of Variation [a] (%)	Mass Concent-ration [a] (mg/mL)	Mean Primary Particle Surface Area [b] (nm^2/particle)	Mean Primary Particle Volume [b] (nm^3/particle)	Theoretical Particle Density [b] (particles/mL)	Theoretical Total Surface Area [b] (mm^2/mL)
8.9	14.7	1.0	249	208	2.58E+14	64277
10.2	16.7	0.9	335	313	1.54E+14	51724
20.3	9.2	1.0	1310	2464	2.18E+13	28506
34.4	10.0	1.0	3750	11989	4.47E+12	16774
41.9	8.6	1.0	5550	21665	2.48E+12	13736
53.1	7.7	1.0	8910	44097	1.22E+12	10835
61.2	8.7	1.0	11800	67511	7.60E+11	8970
67.3	8.0	0.9	14300	89777	5.08E+11	7260
79.8	6.4	1.0	20100	149668	3.58E+11	7202
90.8	8.0	0.9	26000	220485	2.09E+11	5439
99.4	7.0	1.0	31040	289254	1.85E+11	5755
102.3	9.2	1.0	33100	315317	1.70E+11	5630
112.6	6.9	1.0	40000	420471	1.28E+11	5100

2.3 Zebrafish Husbandry and Embryo Collection

Fish water (FW) with a conductivity of 450-510µs was made by dissolving 0.3 g/L Instant Ocean salts (Aquatic Ecosystems, Apopka, FL) in reverse osmosis water and adjusting pH to 7.0-7.4 with sodium bicarbonate (Macron chemicals Phillipsburg, NJ). Adult

zebrafish *Danio rerio* (Tropical D5 strain) were reared in standard laboratory conditions of 28°C with a pH of 7± 0.2 on a 14-h light/10-h dark photoperiod at the Sinnhuber Aquatic Research Laboratory at Oregon State University (Truong et al., 2011). Newly fertilized eggs were collected, rinsed, and placed in fresh FW in a 150-mm plastic petri dish. Viable embryos were housed in an incubator at 28°C in FW on a 16 h light/8 h dark photoperiod in the laboratory until 6 hour post fertilization (hpf).

2.4 Embryo Dechorionation

The dechorionation procedure was adapted from Truong et al. (2011). Pronase (proteinases isolated from *Streptomyces griseus*) was purchased from Sigma-Aldrich (St Louis, MO, USA). Embryos between 6-7 hpf were dechorionated using 64.3 mg/mL protease enzyme. Embryos were incubated for 4-6 minutes with gently swirling, after which the enzyme was removed by rinsing several times (approximately 5 minutes) with fresh FW. Healthy viable embryos between 7-8 hpf were then transferred to a new petri dish with fresh FW just prior to exposure.

2.5 Exposure Method

AgNP stock solution concentrations are listed as mass concentration in Table 1. For each AgNP suspension, stock solutions were diluted in FW by a 4-fold dilution followed by six 5-fold serial dilutions to generate the seven test concentrations (0.061-250 μg/mL) for the dose modeling studies. A 250 mg/L $AgNO_3$ stock solution was prepared in FW on the day of exposure and diluted using six 5-fold serial dilutions. AgNPs and $AgNO_3$ suspensions were loaded into 96-well plates (150μl per well). Twelve individual embryos were exposed at each exposure concentration (one per well) for a total of 96 embryos, including the controls, for each of the thirteen discrete particle sizes.

To investigate the effects of the chorion on embryo toxicity, exposure solutions were prepared by diluting the 8.9 nm AgNPs and 99.4 nm AgNPs stock solutions (1000 mg/L) 2-fold in FW for final concentrations between 5-40 μg/mL. The $AgNO_3$ stock solution (250 mg/L) was diluted in FW 4-fold (0.0098-40 μg/mL). Exposures were performed for each material ($AgNO_3$, 8.9 nm AgNPs, and 99.4 nm AgNPs) for both Ch(+) and Ch(-) embryos. Four experimental replicates were performed for each exposure treatment for a total of 48 individual embryos per treatment (n = 48).

The order of the rows was randomized for each experimental replicate to minimize

potential plate effects. Embryo exposures were initiated following dechorionation, or once the mean age of the embryos reached ~7hpf (between 6hpf and 8hpf) for embryos that were not dechorionated. Embryos exposed to FW alone were included on every plate to provide a control for embryo viability. Embryos were individually exposed to static, nonrenewal treatments, and incubated at 28°C with a 16 h-light/8 h dark photoperiod for the duration of the exposure. All experiments were concluded at 120hpf.

2.6 Zebrafish Embryo Evaluation

The embryo toxicity evaluation procedure used in this study assesses twenty three distinct endpoints corresponding to embryo mortality, dysmorphology, and behavior, which were evaluated at specified time points during development based on those previously described in Truong et al. (2011). Assessments were conducted for every embryo. For exposures designed to investigate the effect of the chorion on embryo toxicity, heart rate at 48 hpf, pericardial edema (PE) at 120 hpf, and mortality at 120 hpf were assessed due to their prevalence during range finding experiments. Embryo heart rate was recorded at 48 hpf for each embryo by counting the number of beats that occurred over a 10-second interval. The presence of PE was evaluated and recorded only for embryos that were still alive at 120 hpf. Embryos were anesthetized during the 120hpf evaluations with 0.5mg/mL of 3-aminobenzoate ethyl ester methanesulfonate salt (tricaine) purchased from Sigma-Aldrich (St Louis, MO, USA). The embryos were humanely euthanized with 2.5mg/mL tricaine at the completion of the 120hpf observations.

2.7 Data Analysis and Statistical Evaluation

Statistical analyses and concentration response modeling were conducted using SigmaPlot™ version 12 (San Jose, CA). Concentration response data were modeled using a three-parameter Logistic function, using global curve fitting and a shared maximum value of 93 (percent survival) to calculate LC_{50} values (Figure 1). The data were also modeled using a four-parameter Logistic function, using global curve fitting and shared maximum and minimum values. LC_{50} values estimated using the four-parameter Logistic function were only considered in regards to Spearman rank correlation described below. The concentration response data were also modeled using the Toxicity Relationship Analysis Program (TRAP), available from the U.S EPA Mid-Continent Ecology Division (TRAP | Mid-Continent Ecology Division | US EPA) to validate the modeling results from the global curve

fitting models. This modeling also used a three-parameter Logistic function but did not use shared values to calculate LC_{50} values and EC_{50} values. Again, LC_{50} values estimated using the EPA TRAP Analysis were only considered in regards to Spearman rank correlation described below.

The relationships between mean primary particle diameter and the estimated LC_{50} values were described using linear regression for each dose metric (Figure 2) and the strength of the relationships were investigated using Spearman rank correlation. Spearman rank correlation is a nonparametric test that measures the association between the two variables based on the order, or "rank" in which the estimated LC_{50} values occurred from most toxic to least toxic in relation to mean primary particle size. The rank for the dependent variable was assigned from low to high with increasing particle diameter and the rank for the independent variable was assigned from low to high with increasing LC_{50} value. The relationship between the ranks of the dependent, and independent variables are statistically significant when associated with a p-value <0.05, and the correlation coefficient (ρ) is a measure of the strength of the association. Correlation coefficient approaching 1 or -1 indicates a strong relationship, a value close to 0 indicates no relationship, and negative coefficients indicate an inverse relationship between the two variables. The Spearman rank correlation was used to analyzed the LC_{50} values estimated using the 3-parameter global curve fitting (SigmaStat), 4-parameter global curve fitting (SigmaStat), and the 3-parameter individually modeled curves (EPA TRAP Analysis).

Mean and standard error for embryo mortality and PE from were calculated from four replicates consisting of twelve embryos per treatment for a total of 48 embryos per treatment group. Mean and standard error were calculated for heart rate by treatment from the complete data set (not between individual experimental replicates) by subtracting the mean of the control animals from each individual value for treated embryos, which were then averaged to calculate the difference from control. One way Analysis of Variance (ANOVA) was used to determine the overall effects of exposure on the dependent variables (mortality, PE, and heart rate). Where effects were shown to be significant ($p < 0.001$), pairwise multiple comparison tests were performed between the means using Holm-Sidak method. Multiple pairwise comparisons were used to identify significant differences from control, difference between Ch (+) and Ch (-) embryos between each material, and within each a material.

Chapter 3: Results

3.1 Dose Modeling and $AgNO_3$ Toxicity

The effect of particle size on embryo mortality was investigated utilizing a suite of AgNPs consisting of thirteen discrete particle sizes ranging between 8.9 nm and 112.6 nm. Theoretical particle characteristics for each of the particles listed in Table 1 are based on the average primary particle diameter measured by TEM and the mass of AgNPs in the stock solution. Embryo mortality at 120hpf was analyzed using nonlinear regression modeling to estimate a LC_{50} value for each particle size. The three-parameter logistic function was found to be the most descriptive and intuitive modeling tool for estimating LC_{50} values. LC_{50} values were estimated using three different dose metrics: mass concentration (μg/L), particle concentration (particles/mL) and surface area concentration (mm^2/mL) (Figure 1). The LC_{50} value for $AgNO_3$ was estimated by mass concentration and resulted in a LC_{50} value that was approximately thirty times lower than the LC_{50} of the smallest AgNP, 0.257 μg/mL as compared to 7.72 μg/mL respectively.

3.2 Size-Dependent Dose Metrics Analysis

When the dose modeling data was analyzed to assess the relationship between embryo survival and mean primary particle size, it was observed that the ordering of the LC_{50} values in Figure 1, from most toxic to lest toxic was significantly different between the three dose metrics, and that the range over which the LC_{50} values occurred also varied considerably. The range of the LC_{50} values estimated by particle concentration covered the largest range where the smallest LC_{50} value ($9.5x10^9$ particles/mL) was two hundred and seventy five times smaller than the largest LC_{50} value ($2.6x10^{12}$ particles/mL). LC_{50} values determined by mass concentration covered the second largest range where the smallest LC_{50} value (8.4 μg/mL) was sixteen times smaller than the largest LC_{50} value (136.1 μg/mL). The LC_{50} values for surface area concentration were distributed over the narrowest range of concentrations, where the smallest LC_{50} value (160.3 mm^2/mL) was only seven and a half times smaller than the largest LC_{50} value (1207.2 mm^2/mL).

Figure 1. Estimated LC_{50} values using three dose metrics. Data points represent the percent survival plotted as a function of, (A) mass concentration, (B) particle concentration, and (C) surface area concentration. The dose-response curves (solid lines) were modeled for each of the thirteen particles sizes for each dose metric. Horizontal dashed lines indicate 50% survival.

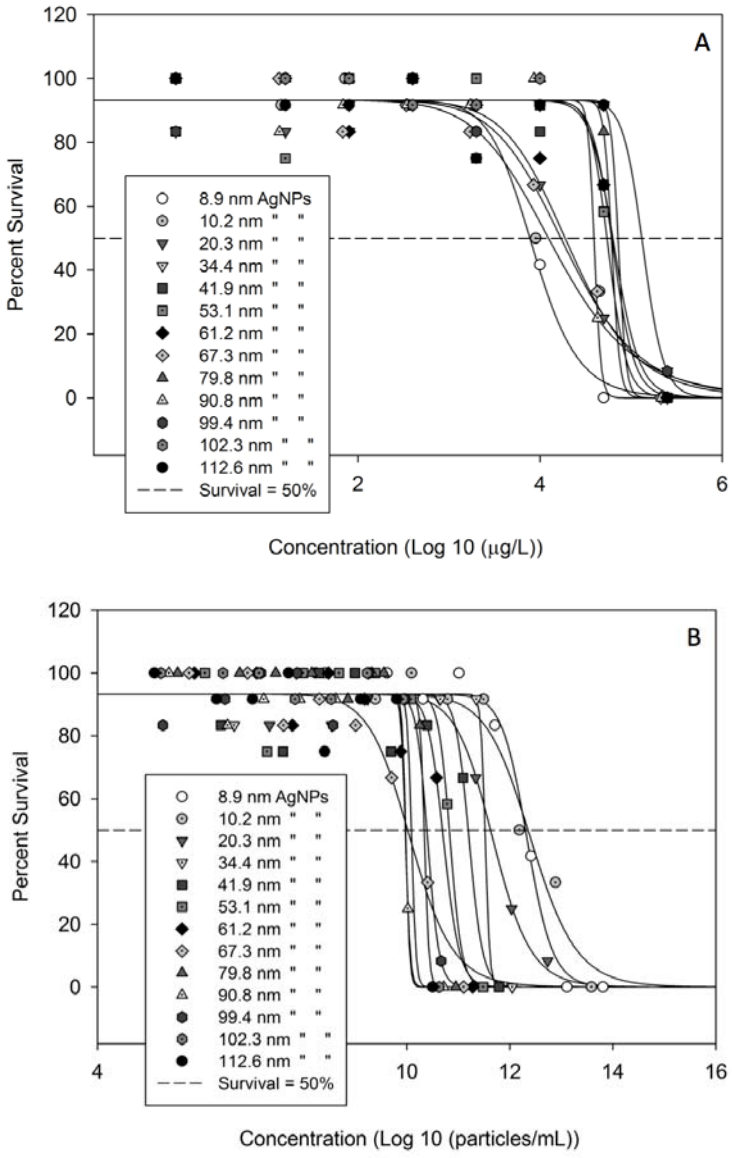

Figure 1. (Continued)

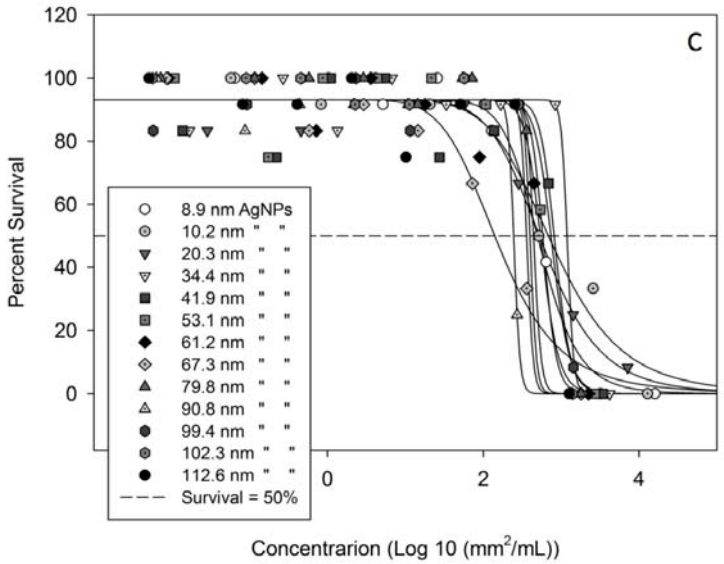

The estimated LC_{50} values for mass concentration (LC_{50} (µg/mL)), particle concentration (LC_{50} (particles/mL)), and surface area concentration (LC_{50} (mm^2/mL)) were plotted against the mean primary particle diameter (Figure 2). Although linear regression analysis was helpful in visually describing the association between the LC_{50} values and particle size, Spearman rank correlation was performed to better understand the relationship between the LC_{50}values and mean primary particle diameter. The Spearman rank correlation coefficients and p-values were similar between the individually modeled curves (EPA TRAP Analysis) and the global curve fitting (SigmaStat, using 3-parameter and 4-parameter Logistic regression) for both mass concentration and particle concentration but were dissimilar for surface area concentration.

Figure 2. Estimated LC_{50} values plotted against mean primary particle diameter for three dose metrics. LC_{50} values are plotted as a function of mean primary particle diameter for (A) mass concentration, (B) particle concentration, and (C) surface area concentration. The best-fit lines from a linear regression analysis are displayed (solid lines) as well as their associated 95%CIs (dashed lines).

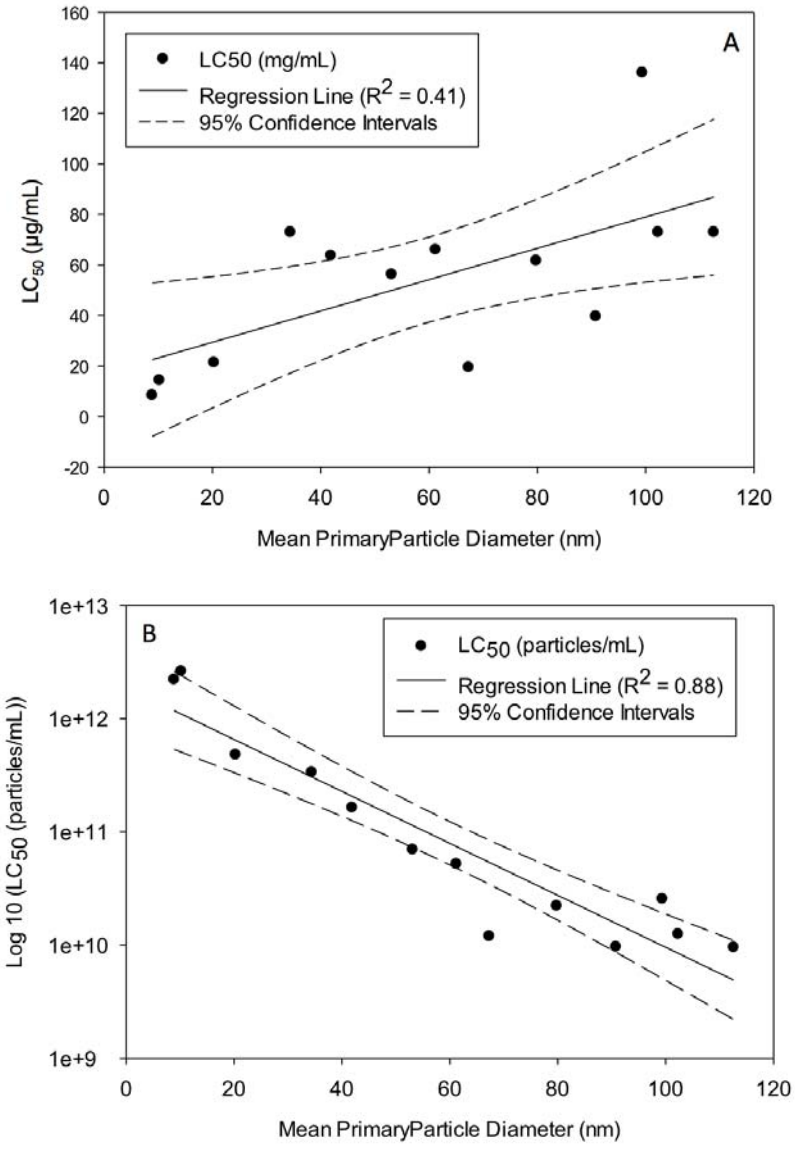

Figure 2. (Continued)

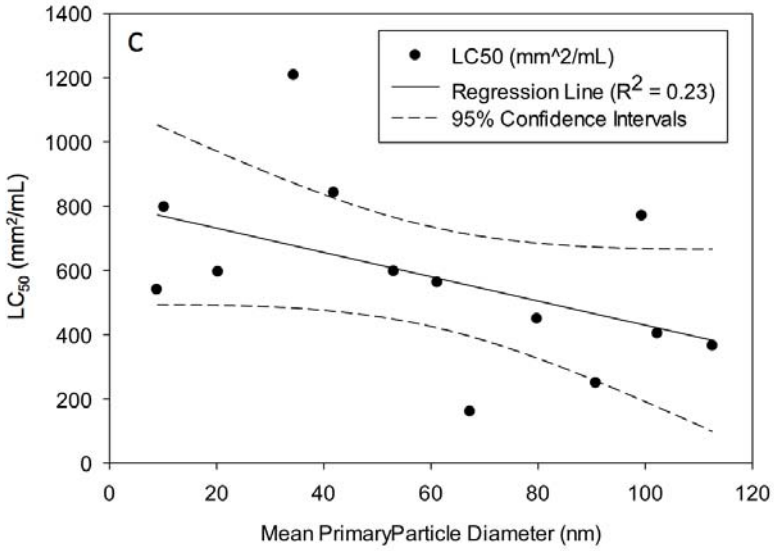

The order of particle sizes from lowest to highest LC_{50} (µg/mL) value, based on mass concentration, using the 3-parameter global curve fitting Logistic regression (SigmaStat), were as follows: 8.9 nm, 10.2 nm, 67.3 nm, 20.3 nm, 90.8 nm, 53.2 nm, 79.8 nm, 41.9 nm, 61.2 nm, 34.4 nm, 102.3 nm, 112.6 nm, and 99.4 nm. The correlation coefficient between LC_{50} (µg/mL) and mean primary particle diameter was (0.652) with a p-value (0.0143), indicating a positive relationship between increasing particle diameter and increasing LC_{50} values. The LC_{50} (µg/mL) values modeled by 4-parameter global curve fitting (SigmaStat) and the 3-parameter individually modeled curves (EPA TRAP Analysis) yielded comparable correlation coefficients of (0.702) and (0.626) with p-values of (0.00651) and (0.0207), respectively.

The order of particle sizes from lowest to highest LC_{50} (particles/mL) value, based on particle concentration, and modeled using the 3-parameter global curve fitting Logistic regression (SigmaStat), were as follows: 112.6 nm, 90.8 nm, 67.3 nm, 102.3 nm, 79.8 nm, 99.4 nm, 61.2 nm, 53.1 nm, 41.9nm, 34.4 nm, 20.3 nm, 8.9 nm, and 10.2 nm. There was a strong inverse correlation (-0.923) between mean primary particle diameter and LC_{50} (particles/mL) with a p-value (< 0.001) for the 3-parameter global curve fitting (SigmaStat) indicating a strong relationship between increasing particle diameter and decreasing LC_{50} values. The values modeled by 4-parameter global curve fitting (SigmaStat), and the 3-

parameter individually modeled curves (EPA TRAP Analysis), yielded very comparable correlation coefficients of (-0.885) and (-0.874) with p-values of (<0.001).

The order of particle sizes from lowest to highest LC_{50} (mm^2/mL) value, based on surface area concentration, and using the 3-parameter global curve fitting Logistic regression (SigmaStat), were as follows: 67.3 nm, 90.8 nm, 112.6 nm, 102.3 nm, 79.8 nm, 8.9 nm, 61.2 nm, 20.3 nm, 53.1 nm, 99.4 nm, 10.2 nm, 41.9 nm, and 34.4 nm. Spearman rank correlation demonstrated a weak inverse correlation (-0.549) between particle diameter and LC_{50} (surface area/mL), with a significant correlation ($p = 0.049$) for the 3-parameter global curve fitting (SigmaStat) indicating a relationship between increasing particle diameter, and decreasing LC_{50} values. In contrast, the values modeled by the 4-parameter global curve fitting (SigmaStat) or the 3-parameter individually modeled curves (EPA TRAP Analysis) generated coefficients of -0.0275 ($p = 0.921$) and -0.390 ($p = 0.179$) respectively, indicating no significant correlation.

3.3 Effect of the Chorion on Embryo Toxicity

The presence of the chorion and its effect on the toxicity of nanomaterials has been demonstrated in previous work (King Heiden et al., 2007). King Heiden et al. (2007) showed that embryos possessing an intact chorion were more sensitive to PAMAM dendrimers at specific time points and concentrations than embryos lacking a chorion. We were therefore interested in the ability of the Ch (+) / Ch (-) variable to act as a contributor to the toxicity of nanomaterials either through enhancement of the mechanism or through a separate mechanism. We exposed Ch (+) and Ch (-) embryos to 10 nm AgNPs, 100 nm AgNPs, and $AgNO_3$ to explore the differences between nano and soluble silver toxicity. Differences between 10 nm AgNPs and 100 nm AgNPs toxicity were compared using alternative does metrics. Results were analyzed using a one-way ANOVA followed by the Holm-Sidak multiple comparisons post hoc test. Significant differences ($p < 0.05$) were observed between control animals and treated animals and between Ch (+) and Ch(-) embryos for mortality, incidence of PE, and heart rate depression. For mortality (Figure 3A), increased toxicity to Ch (+) embryos was observed for 10nm AgNPs, but no differences were observed between Ch (+) and Ch (-) embryos for 100 nm AgNPs or $AgNO_3$ treated embryos. For PE (Figure 4A), increased toxicity to Ch (+) embryos was observed for both 10nm AgNPs and 100 nm AgNPs, but no differences were observed between Ch (+) and Ch (-) embryos treated with $AgNO_3$. For heart rate (Figure 5A), toxicity was greater for Ch (-) embryos

following exposure to 10nm AgNPs, but not 100 nm AgNPs. Concentration dependent differences were observed between Ch (+) and Ch (-) embryos for heat rate depression following exposure to $AgNO_3$ (Figure 5A).

Figure 3. Percent embryo mortality for Ch(+) and Ch(-) embryos when exposed to $AgNO_3$, 8.9 nm AgNP, or 99.4 nm AgNP. The three panels show the same embryo response data plotted as a function of concentration for (A) mass concentration, (B) particle concentration, and (C) surface area concentration. Embryo response data for $AgNO_3$ could only be plotted in panel A, because surface area and particle number calculations do not apply. The mean of four experimental replicates were plotted ± SEM. Symbols represent significant differences between treatments: (a) treated embryos and control embryos for a given material type ($p < 0.05$), and (b) Ch (+) and Ch (-) embryos for a given material type ($p < 0.05$).

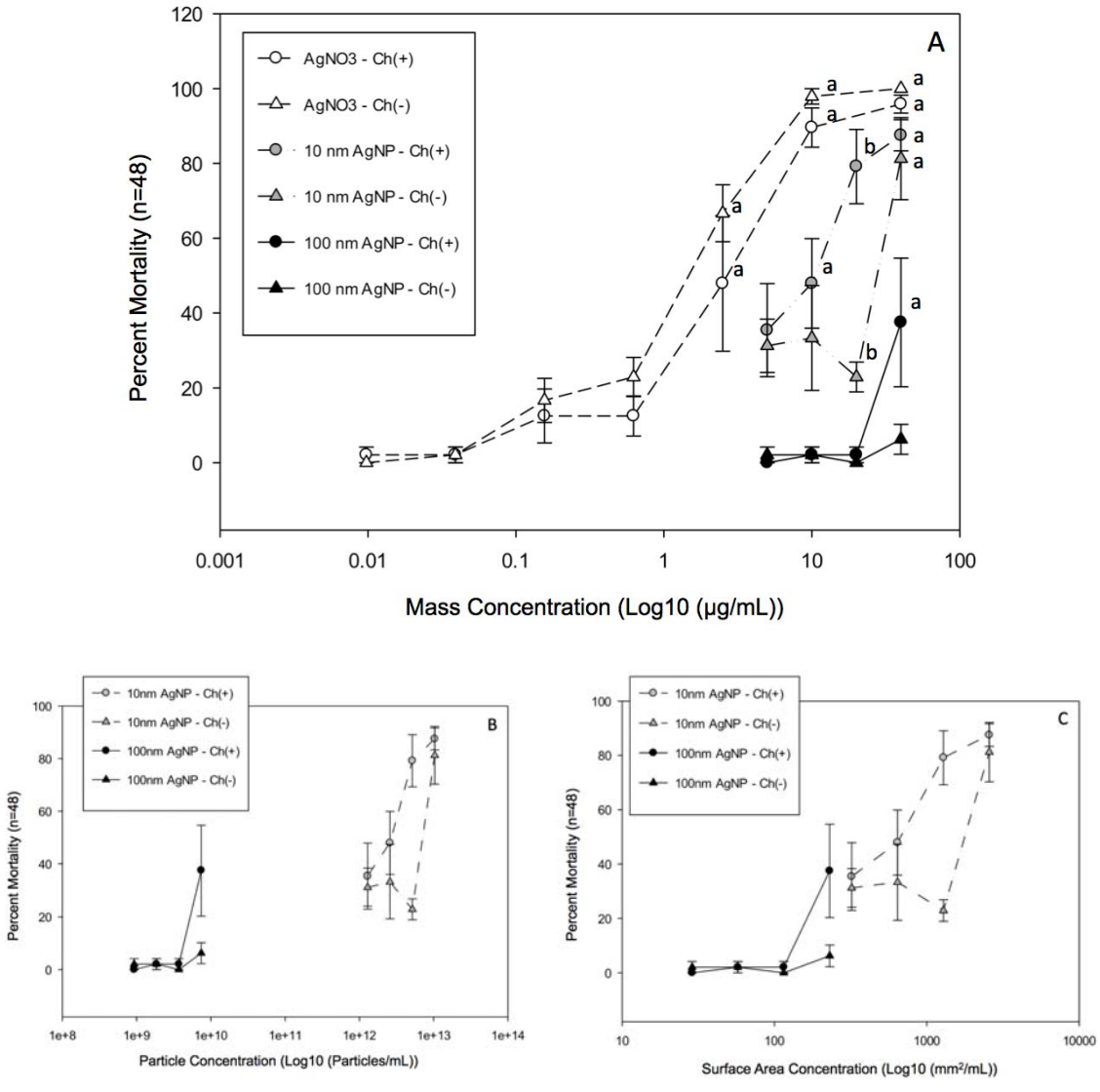

Figure 4: Percent of embryos surviving at 120hpf with PE for Ch(+) and Ch(-) embryos when exposed to $AgNO_3$, 8.9 nm AgNP, or 99.4 nm AgNP. The three panels show the same embryo response data plotted as a function of concentration for (A) mass concentration, (B) particle concentration, and (C) surface area concentration. Embryo response data for $AgNO_3$ could only be plotted in panel A, because surface area and particle number calculations do not apply. The mean of four experimental replicates were plotted ± SEM. Symbols represent differences between treatments: (a) treated embryos and control embryos for a given material type ($p < 0.05$), and (b) Ch (+) and Ch (-) embryos for a given material type ($p < 0.05$).

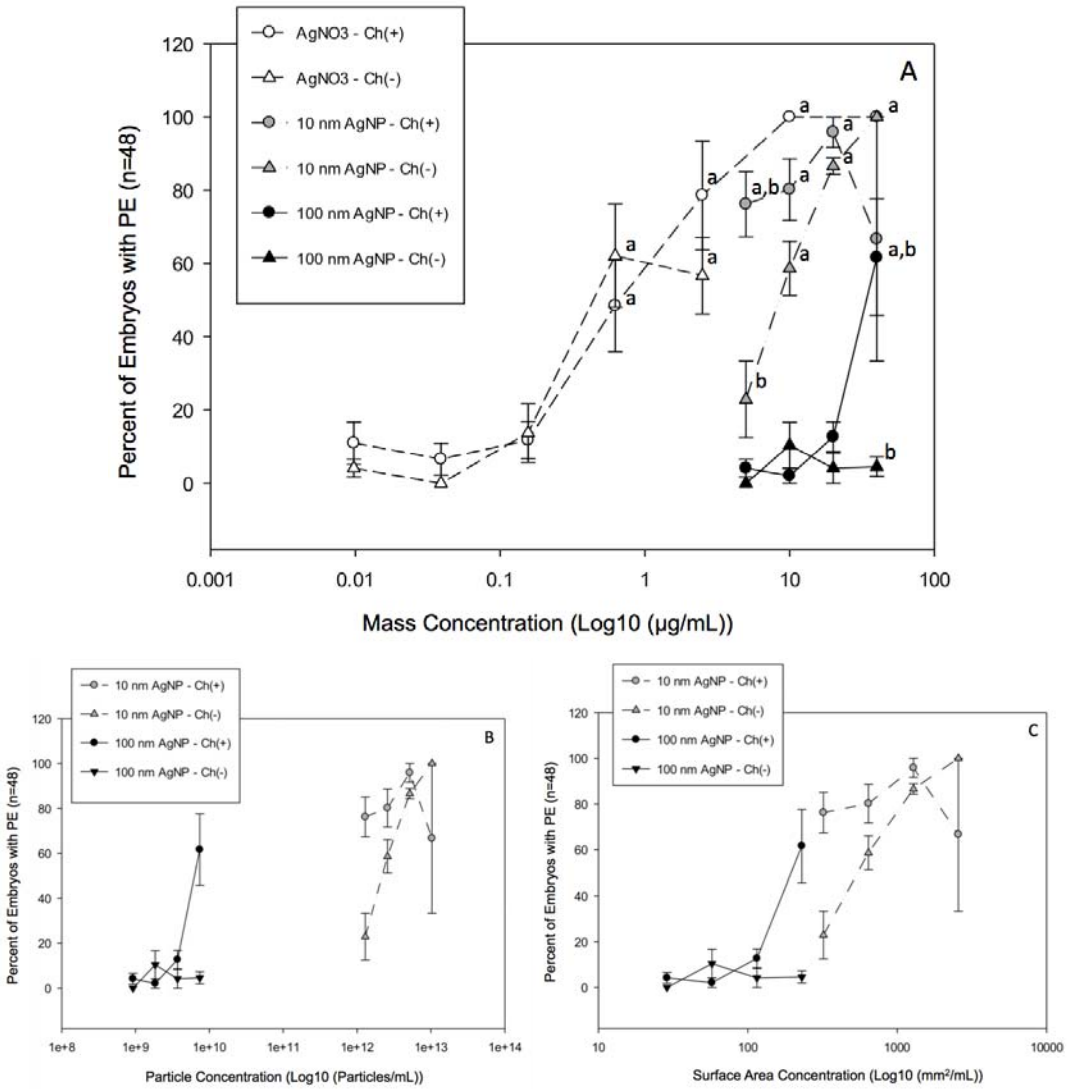

Figure 5. Difference in heart rate from control embryos at 48hpf for Ch(+) and Ch(-) embryos following exposure to $AgNO_3$, 8.9 nm AgNP, or 99.4 nm AgNP. The three panels show the same embryo response data plotted as a function of concentration for (A) mass concentration, (B) particle concentration, and (C) surface area concentration. Embryo response data for $AgNO_3$ could only be plotted in panel A, because surface area and particle number calculations do not apply. The mean of the control animals were subtracted from values of treated embryos to calculate the difference from control. Individual means were then calculated for each experimental replicate. The mean of four experimental replicates were plotted ± SEM. Symbols represent differences between treatments: (a) treated embryos and control embryos for a given material type ($p < 0.05$), and (b) Ch (+) and Ch (-) embryos for a given material type ($p < 0.05$).

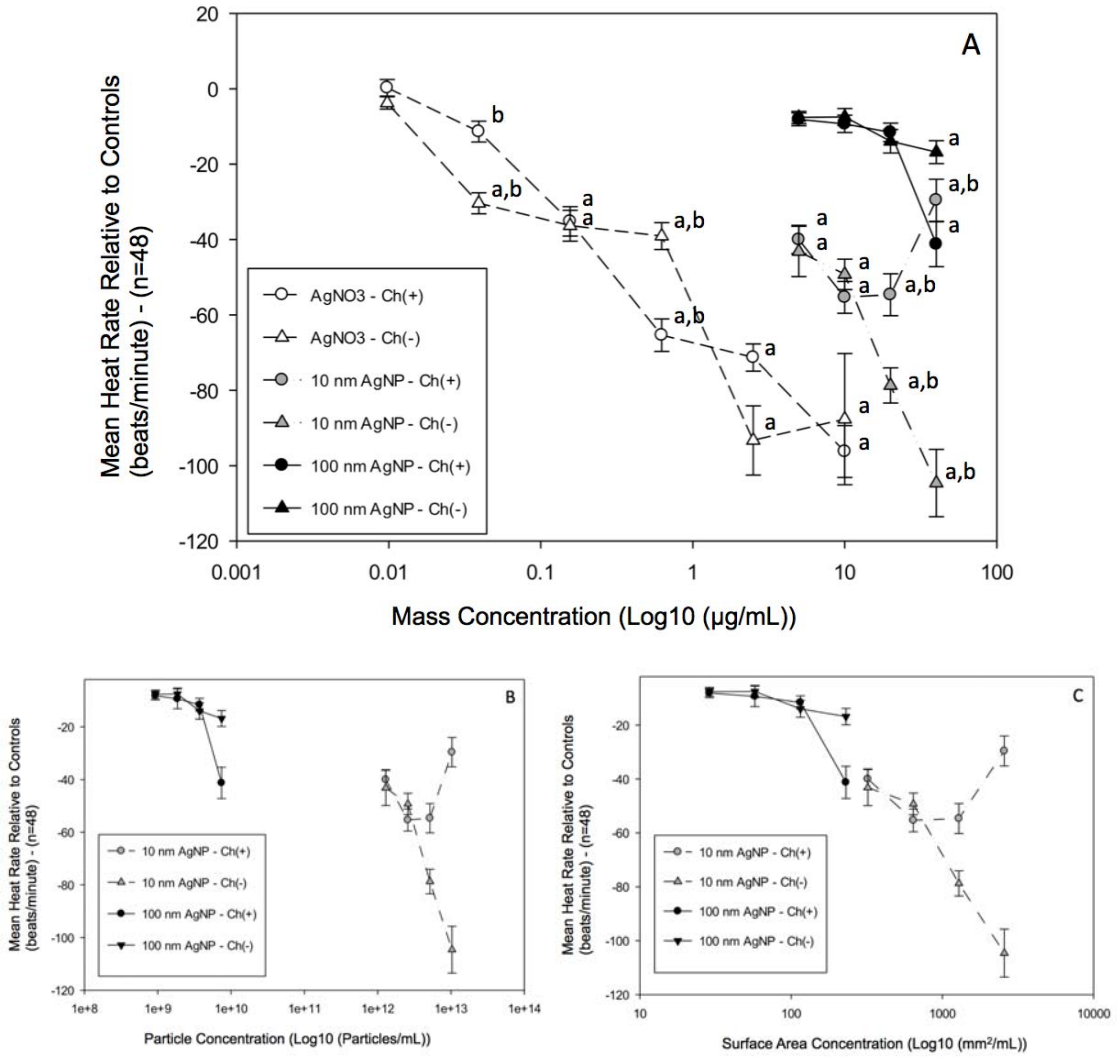

Chapter 4: Discussion

4.1 Overall Findings

The overall findings of this study suggest that the toxicity observed in zebrafish embryos associated with exposure to $AgNO_3$ was very similar to the toxicity observed following exposure to citrate and phosphate stabilized AgNPs. The most sensitive endpoints observed for $AgNO_3$ and AgNPs were decreased heart rate (48 hpf) and incidence of PE (120 hpf), which is consistent with the literature (Asharani et al., 2008; Bar-Ilan et al., 2009). Because of the striking similarity between $AgNO_3$ and AgNP toxicity, AgNP induced toxicity is likely a consequence of AgNP oxidative dissolution and the subsequent release of Ag^+ ions either in solution, or *in vivo*. Embryos were consistently more sensitive to $AgNO_3$ than to AgNPs. The LC_{50} value for $AgNO_3$ (8.4 µg/mL) was found to be approximately thirty times below the LC_{50} value of the most toxic AgNPs by mass concentration. We found that LC_{50} values increased as the mean of the AgNP size distribution increased in approximate order from the smallest mean diameter (8.9 nm) to largest mean diameter (112.6 nm) based on mass concentration. Upon consideration of the two other dose metrics, particle number concentration and surface area concentration, surface area concentration was found to be the exposure metric that best explained the relationship between embryo survival and mean primary particle diameter. We also found that the chorion did increase the toxicity of 10 nm and 100 nm AgNPs, but not $AgNO_3$ ($p<0.05$).

4.2 Overall Characterization of AgNP and $AgNO_3$ Toxicity

The embryo toxicity observed in this study are consistent with those reported by Asharani et al. and other investigations that have shown that AgNPs increased mortality, increased the occurrence of PE, and decreased heart rate in a concentration-dependent manner (Asharani et al., 2008; Bar-Ilan et al., 2009). Other studies have verified that edema and cardiovascular effects are among the most significant effects to zebrafish embryos from exposure to AgNPs (Yeo and Kang, 2008). In the current study, the difference in magnitude between $AgNO_3$ toxicity, and AgNP toxicity was the only difference observed pertaining to embryo response between the materials. This is in general accordance with previous studies that show no significant differences in the presentation of toxicity between $AgNO_3$ and AgNP other than potency (Bar-Ilan et al., 2009; Min-Kyeong Yeo and Jae-Won Yoon, 2009). Specifically, we showed that the most sensitive endpoints for AgNPs and $AgNO_3$ include decreased embryo heart rate and PE, which along with embryo survival, all

displayed similar concentration response relationships. However, according to a mass based dose metric, embryos displayed the greatest sensitivity to $AgNO_3$, followed by 10 nm AgNPs, and were the least sensitive to 100 nm AgNPs for each endpoint measured.

There are many plausible reasons why studies comparing AgNP particle-mediated toxicity and the toxicity associated with exposure to Ag ions are unable to make a distinction between the two. One reason may simply be that the particle-mediated toxicity is significantly lower than the background toxicity induced by silver ions and is therefore difficult to detect. Evidence for this explanation was presented in George et al. (2012) where only silver nano-plates, but not silver nano-spheres, caused toxicity above what was expected from the Ag^+ ions alone. Several other studies show that when dissolved silver ions are removed from nanoparticle suspensions using dialysis or centrifugation techniques, the resulting decrease in the mass of dissolved silver in solution was less than the mass of soluble silver ions ($AgNO_3$) found to cause an equivalent level of toxicity. These findings have prompted several authors to suggest that soluble silver alone could not entirely account for the degree of toxicity observed and that some other mechanism of toxicity must therefore exist to account for the difference (Griffitt et al., 2008a, Griffitt, et al., 2008b; Asharani et al., 2008; George et al., 2012).

We suggest that there are likely two possible reasons why these authors found discrepancies between the observed toxicity and the amount of soluble silver in solution. The first practical explanation is the presence of silver ions sorbed to surface ligands or bare particle surfaces (Liu and Hurt, 2010; Liu et al., 2010). If silver ions are sorbed to the surface of particles and not freely dissolved, the ions may not necessarily be removed under dialysis or centrifugation conditions, but could remain bioavailable. The second explanation is that it is not justified to assume that the dissolved fraction of silver ions in solution is an adequate indication of the dose of silver ions at the site of action and overlooks the possibility that AgNPs are as likely to undergo oxidative dissolution reactions in biological systems as they are in simple aqueous environments. In a simple aqueous environmental system, dissolved molecular oxygen or hydrogen peroxide acts as the oxidizing agents, and the zero-valent silver on the surface of the AgNP is oxidized to produce Ag^+ ions (Liu and Hurt, 2010). When AgNPs undergo oxidative dissolution, some substrate, usually an oxygen containing molecule, must also be reduced and gain an electron to balance out the loss of an electron from the silver atom (Liu and Hurt, 2010; Liu et al., 2010). The process of oxidative dissolution results in the release of Ag^+ ions and subsequent generation of reactive oxygen

intermediates which can lead to further oxidative dissolution (Liu and Hurt, 2010). The same redox reactions that generate Ag+ ions under simple aqueous conditions, could therefore generate ROS in biological systems by reacting with oxygen containing molecules and redox sensitive substrates either on the surface of cells or in intercellular spaces. Intercellular environments have been suggested to accelerate AgNP surface oxidation *in vivo* (AshaRani et al., 2009; Bar-Ilan et al., 2009). In instances where AgNPs could enter intercellular spaces, AgNPs are likely to experience increased rates of dissolution in biological systems as compared to simple environmental systems due to the high concentrations of reactive intermediates. Liu and Hurt (2010) showed that low pH also contributes to AgNP dissolution and therefore, specific intercellular spaces like the lysosome and mitochondria may further increase dissolution due to their low pH and high redox potential respectively. *In vivo* dissolution following uptake and biodistribution could produce relatively high regional concentrations of Ag^{+} ions at the site of action as compared to dissolution in the media. *In vivo* dissolution of AgNPs would also lead to intercellular generation of ROS as a byproduct of dissolution which would further increase AgNP mediated toxicity. Determining whether, and to what extent, AgNPs undergo accelerated oxidative dissolution *in vivo* could explain how studies reporting low ion concentration in solution still result in considerable AgNP toxicity, which exceeds the toxicity that could be attributed to the silver ions alone (Griffitt et al., 2008a; b; Asharani et al., 2008; George et al., 2012). This explanation could also specifically address the findings of George et al. (2012) who found that surface defects on Ag nano-plates produced far greater toxicity than Ag nano-spheres if the combination of shape and surface defects could further accelerate the rate of *in vivo* dissolution resulting in a higher dose at the site of action.

Despite the presence of metal ions in colloidal and nanomaterial suspensions that undoubtedly contribute significantly to the toxicity of many ENMs, understanding the surface-mediated toxicity, which encompasses oxidative dissolution, is fundamental to understanding ENM toxicity. In all likelihood, AgNP associated toxicity is due to the chemical process of oxidative dissolution, which generates ions and ROS. Liu et al. (2010) provide some support for this hypothesis by showing that the antimicrobial activity of nanosilver can be increased or eliminated completely by directly controlling the rate of dissolution using AgNP surface treatment. The inherent instability and reactivity of many ENMs needs to be carefully evaluated to account for potential effects on living systems in the context of metal ion toxicity and its relationship to reactive surface area. The toxicity of

several ENMs is likely a result of this interconnected process, linking particle mediated surface reactivity and ion mediated toxicity. This represents as unified mechanisms of action in which both processes are occurring simultaneously as a result of oxidative dissolution, liberating ions and generating reactive oxygen species in a surface area dependent manner. This hypothesis will need to be tested directly with future studies that address this question in a material-specific manner and one that attempts to distinguish between the reactivity of the particle surface and the innate toxicity of the ions *in vivo*.

4.3 Presence of the Chorion Effects AgNP Toxicity

In preliminary work investigating the toxicity of AgNPs, we observed that the toxicity of 10 nm and 100 nm AgNPs was greater to Ch(+) embryos than to Ch(-) embryos and nanoparticles were observed covering the surface of the chorion. We wanted to learn how the chorion might act as a barrier to AgNPs, but still result in increased toxicity. To explore if the chorion enhanced toxicity is specific to ENMs, we tested whether Ch(+) and Ch(-) embryos exposed to $AgNO_3$ would also result in a significant difference in toxicity. The literature suggests that dissolved Ag+ ions would move freely in and out of the chorion where as AgNPs movement could be restricted or hindered. As we had previously observed, the toxicity of 10 nm and 100 nm AgNPs was found to be greater in Ch(+) embryos than in Ch(-) embryos at some test concentrations. In contrast to the AgNPs, and in support of our hypothesis, we did not observe a significant increase in toxicity for Ch(+) embryos exposed to $AgNO_3$ versus Ch(-) embryos. This suggests an additional nano-mediated effect not observed in relation to the freely dissolved metal.

In support of this, Lee et al. (2007) showed that AgNPs can become trapped in the chorionic pore space and that pores can be blocked by agglomerates. By blocking pores, ENMs could potentially decrease gas exchange across the chorionic surface by clogging the chorionic canals and effectively creating hypoxic conditions in the inner chorionic space causing increased toxicity. This could help to explain the increase in toxicity observed in chorinated versus dechorionated embryos following exposure to AgNPs and might also account for the lack of a difference in toxicity for $AgNO_3$ exposures (Figure 3,4,5). Other studies have shown that the chorion can actively accumulate metal ions in the perivitelline fluid following exposure to metal oxide nanoparticles at higher concentrations than in the sounding media (Xia et al., 2011; Lin et al., 2011). This is thought to be due to the presence of several proteins within the chorionic fluid that may bind and sequester metals (Xia et al.,

2011; Lin et al., 2011). Other studies have shown that some ENMs including ZnO nanoparticles may inhibit the activity of the zebrafish hatching enzyme (ZHE1) which could in some cases lead to decreased survival (Xia et al., 2011; Lin et al., 2011).

In combination with previously published literature, the studies presented here demonstrate the capacity of the chorion to enhance toxicity for specific ENMs. While removing the chorion may increase toxicity by allowing for direct exposure to some materials, for other materials chorion removal may actually underestimate the toxic potential of some ENMs whose mechanism of action may be enhanced by or rely on the presence of a chorion. More work is clearly needed to determine the mechanisms by which chorions increase the toxicity of ENMs.

4.4 Dose Metrics Considerations for AgNPs

In nanotoxicology, alternate metrics for exposure and dose are needed to fully understand toxicity associated with particle characteristics (Oberdörster et al., 2005; Teeguarden et al., 2007). However, using alternative dose and exposure metrics challenges the traditional way we measure the toxicity of materials and the way we classify hazards. In contrast to conventional small molecules, where most exposure variables are closely proportional to one another, exposure variables do not usually scale linearly for nanomaterials, but more often scale exponentially due to their three-dimensional shape. This study illustrates why alternative dose metrics matter when characterizing the toxicity of ENMs. This study shows that the dose metrics chosen for nanotoxicology data analysis can have a drastic influence on the interpretation of the study findings. We conclude that particle concentration and surface area concentrations are more valuable estimators for silver nanoparticle toxicity than conventional mass based dose metrics and that the observed size-dependent toxicity of spherical AgNPs is due specifically to surface area.

Specifically, our analyses illustrate that smaller AgNP size distributions have lower LC_{50} (μg/mL) values and therefore appear to be more toxic to embryos than larger particles, given equivalent masses. In contrast, when the theoretical number of particles in solution is considered, larger AgNP size distributions are associated with lower LC_{50} (particles/mL) values, and therefore appear to be far more toxic than smaller particles on a per particle basis. When the toxicity is considered as a function of the combined surface area of the particles in solution, the difference in LC_{50} (mm^2/mL) values is minimized and larger particles appear to be less than a factor of ten times more toxic than smaller particles. The

results of the Spearman rank correlation analysis demonstrated that the correlation between the mean primary particle size for both mass concentration and particle concentration appear to be stronger than for surface area concentration. We determined that this was because the calculation for estimating surface area concentration factors out particle number. Factoring out particle number effectively eliminates the variable that is most influenced by differences in primary particle size and the variable with the greatest range of values. In contrast, particle number is not factored out for mass concentration and particle number concentration. This is the reason that mass concentration and particle number concentration exhibit clear size-dependent relationships. With decreasing particle diameter, particle number and surface area per particle both vary exponentially but in opposite directions and at disproportionate rates; particle number will increase rapidly as diameter decreases and surface area per particle will decrease at a slower rate. When considering equivalent masses, a smaller particle size distribution will have an exponentially greater particle concentration than the particle concentration for a larger size distribution. As a consequence of the disproportionate rate change for these two variables, smaller particle size distribution will also have a much greater total surface area. The fact that small particle size distribution will have an exponentially greater surface area concentration given an equivalent mass helps to explain why our original observations and many other nanotoxicology studies that only report mass based concentration, also report that smaller size distributions are more toxic to organisms than larger size distributions. Because particle number increases more quickly than surface area decreases with decreasing particle size, it takes a smaller mass of smaller particles to reach the effective surface area dose than it does for larger particles, despite the fact that larger particles have far more surface area per particle than smaller particles. This study has found that when particle number is nominalized to derive surface area values, the result is a narrow range of surface area concentrations that cause equivalent mortality for AgNPs ranging from 8.9 nm to 112.6 nm. For this reason, we suggest that total surface area concentration best represents the physical feature of the AgNPs that is responsible for eliciting toxicity in embryonic zebrafish.

Work by Sotiriou et al. (2011) investigating the antimicrobial activity of Ag/silica nanoparticles utilized the same three alternative dose metrics (Ag surface area concentration, Ag mass concentration, and Ag particle number concentration) in their study and showed that antimicrobial activity was most strongly correlated with Ag specific

surface area (R^2 =0.90). Sotiriou et al., (2011)also observed that the relationship between antimicrobial activity and mass concentration (R^2 =0.56) provided the weakest correlation. The authors suggested that that relying on mass based dose metrics imposes limitations on understanding the antibacterial activity of nanosilver (Sotiriou et al., 2011). This study the and study by Sotiriou et al., suggest that surface area concentration is a more accurate predictor of nanosilver mediated toxicity, and that mass concentration is the most misleading of the three dose metrics because it inadequately represents the three dimensional nature of the particles. However, our current paradigm for dose response is limited to mass based measures.

Targeted dose response modeling was not conducted for each material because the dose modeling data used in this study was initially intended only as a tier-1 hazard identification and range finding study. As a result, the actual concentration response area of the curves occurred over the highest four concentrations for all of the AgNPs tested, with fewer than four concentrations represented in the dose response region for the largest particle size distributions. Despite this limitation, by systematically varying particle diameter across a large number of distinct particle suspensions with narrow size distributions, the data from the dose modeling experiments clearly show size dependent toxicity of AgNPs to zebrafish embryos.

The importance of choosing appropriate dose metrics in nanotoxicology was also illustrated by the dose metric analyses for the Ch(+) / Ch(-) embryo response data. The concentrations tested in the Ch(+) / Ch(-) exposures were selected to represent equivalent mass based concentrations (µg/mL) and are therefore overlapping. Alternative dose metrics were not, however, taken into consideration at the time the exposure concentrations were selected. Consequently, when the embryo response was plotted by particle concentration (particles/mL) or by surface area concentration (mm^2/mL), the embryo responses no longer occur over a shared range of concentrations and were therefore no longer directly comparable. This observation helped to qualitatively verify the findings from the dose metric analysis from the dose modeling results. Alternative dose metrics are a valuable tool for making comparisons between the relative potency of different ENMs and whether observed differences are real, or artifacts of study design and/ or data analysis. Although retrospective alternative dose metrics analyses of nanotoxicology data is possible, it is less likely to be informative, reiterating the importance of designing studies with alternative dose metrics in mind.

Chapter 5: Conclusions

In this study, we have compared three of the most common alternative dose metrics to describe nanomaterial toxicity: surface area, particle number, and mass. We found that concentration based on total surface area was the most informative and the most appropriate dose metric for describing AgNP mediated embryo toxicity. Although the concept that surface area is a driving factor in nanoparticle mediated toxicity has been previously proposed (Oberdörster et al., 2005), the data presented here provide strong support for this generally hypothesized relationship by linking theoretical nanoparticle surface area to an *in vivo* biological response. The importance of surface area as a dose metric for toxicology studies may be of equally great importance for both metal nanomaterials and significantly larger bulk materials in relation to their aqueous dissolution. Liu et al. demonstrated this by comparing the dissolution rates between 4.8 nm spherical AgNPs, 60nm triangular AgNPs and a 1 mm macroscopic silver foil which all released Ag^{+} ions at a similar rate on the basis of surface area, but not on a mass basis (Liu et al., 2010). This implies that dissolution is a function of the elemental properties of the material itself as opposed to inherent nano-scale properties.

The importance of surface area as the primary determinant and predictor of toxicity in relation to the dissolution of non-nanoscale metals and metal alloys has also been previously observed. Metals, including metal powders, produced for commercial purposes are subject to regulation based on hazard identification and classification. One component of metal powder hazard characterization involves a standard laboratory technique referred to as a transformation/dissolution protocol (T/DP). The procedure is used to measure the rate of dissolution and the release of ions and other bioavailable metal species in environmentally relevant aqueous medium by sampling the soluble fraction over time which can then be compared to acute toxicity data to characterize the inherent hazard (Skeaff et al., 2000, 2009). Skeaff et al. (2009) explains that according to the Global Harmonization System's hazard classifacation system, metal coumpounds with ecotoxicity values (LC_{50} or EC_{50}) that are above 100 mg/L would need no further hazard classification but compounds with LC_{50} or (EC_{50}) values below 100 mg/L would require analysis using a T/DP to assess the release of disolved metal (Skeaff et al., 2009). Based on this classification system, particle/grain size could significantly impact the hazard classification unless surface area is accounted for. Skeaff and colleagues have therfore defined the critical surface area (CSA) as the surface area per liter, or metal alloy that will result in a mass of

dissolved metal that is equal to the LC_{50} (or EC_{50}) value for the metal's soluble salt and estimated using a relevant test organism with a standard toxicity assay (Skeaff et al., 2000). CSA can be based on calculated or measured surface areas (Skeaff et al., 2000). CSA derived toxicity is dependent on the inherent properties of the material, including its ability to undergo dissolution, its tendency to form of stable ionic species in solution, and the toxicity of the ionic species. Because the surface area directly influences the dissolution rate of dissolution per unit mass, it subsequently influences the apparent toxicity. We suggest that the toxicity associated with spherical AgNPs is also dominated by the release of ionic silver through oxidative dissolution in solution. Figure 7 shows three schematic representations that illustrate the different dose metrics and how they relate to embryo toxicity in the context of this study and the concept of CSA.

Figure 6. Conceptual diagram summarizing the importance of surface area as a dose metric for nanomaterials. Relationships observed between embryo toxicity and (A) mass based concentration, (B) particle number based concentration, and (C) surface area based concentration. The flat line indicates very narrow range of surface area concentrations that approximate a single CSA concentration.

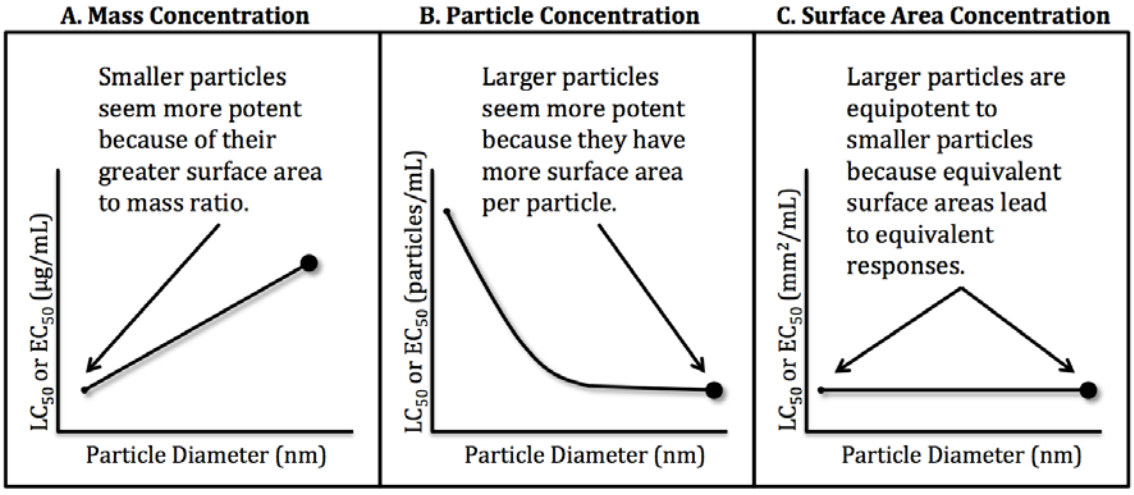

The relationship between embryo toxicity and mass concentration (Figure 7A) shows that smaller diameter particles are more toxic due to a larger surface area to mass

ratio. Smaller particles, therefore, reach a CSA concentration at lower mass than larger diameter particles, which have less surface area per mass. The relationship between embryo toxicity and particle concentration (Figure 7B) shows that larger diameter particles are more toxic to embryos because larger particles have more surface area per particle than smaller particles. Therefore, it takes fewer larger diameter particles to reach the CSA concentration. Lastly, the relationship between embryo toxicity and surface area concentration (Figure 7C) shows that larger particles are not significantly more or less toxic to embryos than smaller particles. This is because embryo mortality is dependent upon a single CSA concentration.

More work is required to understand the role of surface area mediated effects and their role in AgNP toxicity. Nanoparticle surface area mediated toxicity is of significant importance from a regulatory perspective because of potential implications regarding human exposure and our current mass based paradigm for hazard assessment. Understanding the surface area mediated effects of ENMs is important because many other metallic nanomaterials including copper, aluminum, cobalt, and nickel undergo dissolution (Griffitt et al., 2008b). Nanomaterial dissolution and inherent instability could constitute a common mechanism of toxicity for metallic nanomaterials. It remains unknown if the toxicity of AgNPs is due only to the surface area dependent release of silver ions, or if cell surfaces and interiors can react directly with AgNP surfaces, resulting in ROS generation and damage to cellular components. Very likely, both forms of toxicity are occurring simultaneously. Evidence supporting this hypothesis is based on the understanding that silver ions are acutely toxic to aquatic life. Additionally AgNPs are known to undergo considerable oxidative dissolution in aquatic environments and oxidative dissolution both generates ROS and is accelerated by ROS.

Our working hypothesis is that it is not the ions alone that cause toxicity but rather, the oxidative dissolution of the AgNPs that generates both silver ions and ROS. Recent studies support this hypothesis, showing a size dependent increase in intercellular ROS generation and growth inhibition in nitrifying bacteria as particle size distributions (average size 9-21 nm) were shifted toward increasing numbers of smaller (≤ 5nm) AgNPs (Choi and Hu, 2008). Although there is still limited knowledge regarding potential *in vivo* and intercellular ROS generation from the oxidative dissolution of AgNPs, it seems plausible that silver ions themselves are responsible for the majority of the toxicity observed in aquatic animal models.

Nanomaterial SARs and alternative dose metrics have the potential to uncover important chemical and structural relationships and interactions between nanomaterials and biological systems and to predict the behavior of future materials. This work reports on a systematic evaluation of AgNPs based on size and has yielded a physicochemical SAR between average AgNP size and embryo mortality. This study underscores the importance of using a systematic approach in nanotoxicology studies. The AgNPs used in this study were well characterized, well dispersed, and had narrow size distributions. Without accurate characterization information and tight control over material properties, it is difficult to move away from reporting results, and move toward making informed conclusions about the relationships between nanomaterial structural properties and the biological response they elicit.

A fundamental objective of nanotoxicology is to understand the physicochemical properties that ultimately lead to toxicity. For this reason, a combination of high throughput assays, high quality material characterization, and modeling strategies are needed to advance the science of nanotoxicology and clearly understand the potential hazards, inherent risks, and environmental fate of ENMs. It is important for nanotoxicology studies to move away from conventional dose metrics (i.e. mass based dose metrics) and to utilize dose metrics that account for the three-dimensional shape of nanomaterials (i.e. surface area, volume, and particle number dose metrics). Analogous to the work defining the CSA for metals and metal alloys by Skeaff et al. (Skeaff et al., 2000) it will be interesting to see how alternative dose metrics will be incorporated into nanomaterial risk assessment frameworks and hazard characterization in the future.

References

Ahamed, M., R. Posgai, T.J. Gorey, M. Nielsen, S.M. Hussain, and J.J. Rowe. 2010. Silver nanoparticles induced heat shock protein 70, oxidative stress and apoptosis in Drosophila melanogaster. *Toxicology and Applied Pharmacology*. 242:263–269.

AshaRani, P.V., G. Low Kah Mun, M.P. Hande, and S. Valiyaveettil. 2009. Cytotoxicity and Genotoxicity of Silver Nanoparticles in Human Cells. *ACS Nano*. 3:279–290.

Asharani, P.V., Y. Lian Wu, Z. Gong, and S. Valiyaveettil. 2008. Toxicity of silver nanoparticles in zebrafish models. *Nanotechnology*. 19:255102.

Bar-Ilan, O., R.M. Albrecht, V.E. Fako, and D.Y. Furgeson. 2009. Toxicity Assessments of Multisized Gold and Silver Nanoparticles in Zebrafish Embryos. *Small*. 5:1897–1910.

Benn, T., B. Cavanagh, K. Hristovski, J.D. Posner, and P. Westerhoff. 2010. The Release of Nanosilver from Consumer Products Used in the Home. *Journal of Environment Quality*. 39:1875.

Bowman, C.R., F.C. Bailey, M. Elrod-Erickson, A.M. Neigh, and R.R. Otter. 2012. Effects of silver nanoparticles on zebrafish (Danio rerio) and Escherichia coli (ATCC 25922): A comparison of toxicity based on total surface area versus mass concentration of particles in a model eukaryotic and prokaryotic system. *Environmental Toxicology and Chemistry*. 31:1793–1800.

Carlson, C., S.M. Hussain, A.M. Schrand, L. K. Braydich-Stolle, K.L. Hess, R.L. Jones, and J.J. Schlager. 2008. Unique Cellular Interaction of Silver Nanoparticles: Size-Dependent Generation of Reactive Oxygen Species. *The Journal of Physical Chemistry B*. 112:13608–13619.

Chen, X., and H.J. Schluesener. 2008. Nanosilver: A nanoproduct in medical application. *Toxicology Letters*. 176:1–12.

Choi, J.E., S. Kim, J.H. Ahn, P. Youn, J.S. Kang, K. Park, J. Yi, and D.-Y. Ryu. 2010. Induction of oxidative stress and apoptosis by silver nanoparticles in the liver of adult zebrafish. *Aquatic Toxicology*. 100:151–159.

Choi, O., and Z. Hu. 2008. Size Dependent and Reactive Oxygen Species Related Nanosilver Toxicity to Nitrifying Bacteria. *Environmental Science & Technology*. 42:4583–4588.

Georgantzopoulou, A., Y.L. Balachandran, P. Rosenkranz, M. Dusinska, A. Lankoff, M. Wojewodzka, M. Kruszewski, C. Guignard, J.-N. Audinot, S. Girija, L. Hoffmann, and

A.C. Gutleb. 2012. Ag nanoparticles: size- and surface-dependent effects on model aquatic organisms and uptake evaluation with NanoSIMS. *Nanotoxicology*. 1–11.

George, S., S. Lin, Z. Ji, C.R. Thomas, L. Li, M. Mecklenburg, H. Meng, X. Wang, H. Zhang, T. Xia, J.N. Hohman, S. Lin, J.I. Zink, P.S. Weiss, and A.E. Nel. 2012. Surface Defects on Plate-Shaped Silver Nanoparticles Contribute to Its Hazard Potential in a Fish Gill Cell Line and Zebrafish Embryos. *ACS Nano*. 6:3745–3759.

George, S., T. Xia, R. Rallo, Y. Zhao, Z. Ji, S. Lin, X. Wang, H. Zhang, B. France, D. Schoenfeld, R. Damoiseaux, R. Liu, S. Lin, K.A. Bradley, Y. Cohen, and A.E. Nel. 2011. Use of a High-Throughput Screening Approach Coupled with In Vivo Zebrafish Embryo Screening To Develop Hazard Ranking for Engineered Nanomaterials. *ACS Nano*. 5:1805–1817.

Griffitt, R.J., K. Hyndman, N.D. Denslow, and D.S. Barber. 2008a. Comparison of Molecular and Histological Changes in Zebrafish Gills Exposed to Metallic Nanoparticles. *Toxicological Sciences*. 107:404–415.

Griffitt, R.J., J. Luo, J. Gao, J.C. Bonzongo, and D.S. Barber. 2008b. Effects of particle composition and species on toxicity of metallic nanomaterials in aquatic organisms. *Environmental Toxicology and Chemistry*. 27:1972–1978.

Harper, S., C. Usenko, J. Hutchison, B. Maddux, and R. Tanguay. 2008a. In vivo biodistribution and toxicity depends on nanomaterial composition, size, surface functionalization and route of exposure. *Journal of Experimental Nanoscience*. 3:195–206.

Harper, S.L., J.L. Carriere, J.M. Miller, J.E. Hutchison, B.L.S. Maddux, and R.L. Tanguay. 2011. Systematic Evaluation of Nanomaterial Toxicity: Utility of Standardized Materials and Rapid Assays. *ACS Nano*. 5:4688–4697.

Harper, S.L., J.A. Dahl, B.L.S. Maddux, and R.L. Tanguay. 2008b. Proactively designing nanomaterials to enhance performance and minimise hazard. *International Journal of Nanotechnology*. 5:124–142.

Hwang, E.T., J.H. Lee, Y.J. Chae, Y.S. Kim, B.C. Kim, B.-I. Sang, and M.B. Gu. 2008. Analysis of the Toxic Mode of Action of Silver Nanoparticles Using Stress-Specific Bioluminescent Bacteria. *Small*. 4:746–750.

King Heiden, T.C., E. Dengler, W.J. Kao, W. Heideman, and R.E. Peterson. 2007. Developmental toxicity of low generation PAMAM dendrimers in zebrafish. *Toxicology and Applied Pharmacology*. 225:70–79.

Kittler, S., C. Greulich, J. Diendorf, M. Köller, and M. Epple. 2010. Toxicity of Silver Nanoparticles Increases during Storage Because of Slow Dissolution under Release of Silver Ions. *Chemistry of Materials*. 22:4548–4554.

Lee, K.J., P.D. Nallathamby, L.M. Browning, C.J. Osgood, and X.-H.N. Xu. 2007. In Vivo Imaging of Transport and Biocompatibility of Single Silver Nanoparticles in Early Development of Zebrafish Embryos. *ACS Nano*. 1:133–143.

Lee, Y.-J., J. Kim, J. Oh, S. Bae, S. Lee, I.S. Hong, and S.-H. Kim. 2012. Ion-release kinetics and ecotoxicity effects of silver nanoparticles. *Environmental Toxicology and Chemistry*. 31:155–159.

Lin, S., Y. Zhao, T. Xia, H. Meng, Z. Ji, R. Liu, S. George, S. Xiong, X. Wang, H. Zhang, S. Pokhrel, L. Mädler, R. Damoiseaux, S. Lin, and A.E. Nel. 2011. High Content Screening in Zebrafish Speeds up Hazard Ranking of Transition Metal Oxide Nanoparticles. *ACS Nano*. 5:7284–7295.

Liu, J., and R.H. Hurt. 2010. Ion Release Kinetics and Particle Persistence in Aqueous Nano-Silver Colloids. *Environmental Science & Technology*. 44:2169–2175.

Liu, J., D.A. Sonshine, S. Shervani, and R.H. Hurt. 2010. Controlled Release of Biologically Active Silver from Nanosilver Surfaces. *ACS Nano*. 4:6903–6913.

Lok, C.-N., C.-M. Ho, R. Chen, Q.-Y. He, W.-Y. Yu, H. Sun, P.K.-H. Tam, J.-F. Chiu, and C.-M. Che. 2007. Silver nanoparticles: partial oxidation and antibacterial activities. *JBIC Journal of Biological Inorganic Chemistry*. 12:527–534.

Ma, R., C. Levard, S.M. Marinakos, Y. Cheng, J. Liu, F.M. Michel, G.E. Brown, and G.V. Lowry. 2012. Size-Controlled Dissolution of Organic-Coated Silver Nanoparticles. *Environmental Science & Technology*. 46:752–759.

Meyer, J.N., C.A. Lord, X.Y. Yang, E.A. Turner, A.R. Badireddy, S.M. Marinakos, A. Chilkoti, M.R. Wiesner, and M. Auffan. 2010. Intracellular uptake and associated toxicity of silver nanoparticles in Caenorhabditis elegans. *Aquatic Toxicology*. 100:140–150.

Min-Kyeong Yeo, and Jae-Won Yoon. 2009. Comparison of the Effects of Nano-silver Antibacterial Coatings and Silver Ions on Zebrafish Embryogenesis.

Navarro, E., F. Piccapietra, B. Wagner, F. Marconi, R. Kaegi, N. Odzak, L. Sigg, and R. Behra. 2008. Toxicity of Silver Nanoparticles to Chlamydomonas reinhardtii. *Environmental Science & Technology*. 42:8959–8964.

Nel, A. 2006. Toxic Potential of Materials at the Nanolevel. *Science*. 311:622–627.

Nel, A., T. Xia, H. Meng, X. Wang, S. Lin, Z. Ji, and H. Zhang. 2012. Nanomaterial Toxicity Testing in the 21st Century: Use of a Predictive Toxicological Approach and High-Throughput Screening. *Accounts of Chemical Research*. 120607141248005.

Oberdörster, G., A. Maynard, K. Donaldson, V. Castranova, J. Fitzpatrick, K. Ausman, J. Carter, B. Karn, W. Kreyling, D. Lai, and others. 2005. Principles for characterizing

the potential human health effects from exposure to nanomaterials: elements of a screening strategy. *Particle and Fibre Toxicology*. 2:8.

Park, E.-J., J. Yi, Y. Kim, K. Choi, and K. Park. 2010. Silver nanoparticles induce cytotoxicity by a Trojan-horse type mechanism. *Toxicology in Vitro*. 24:872–878.

Park, J., D.-H. Lim, H.-J. Lim, T. Kwon, J. Choi, S. Jeong, I.-H. Choi, and J. Cheon. 2011a. Size dependent macrophage responses and toxicological effects of Ag nanoparticles. *Chemical Communications*. 47:4382.

Park, M.V.D.Z., A.M. Neigh, J.P. Vermeulen, L.J.J. de la Fonteyne, H.W. Verharen, J.J. Briedé, H. van Loveren, and W.H. de Jong. 2011b. The effect of particle size on the cytotoxicity, inflammation, developmental toxicity and genotoxicity of silver nanoparticles. *Biomaterials*. 32:9810–9817.

Piao, M.J., K.A. Kang, I.K. Lee, H.S. Kim, S. Kim, J.Y. Choi, J. Choi, and J.W. Hyun. 2011. Silver nanoparticles induce oxidative cell damage in human liver cells through inhibition of reduced glutathione and induction of mitochondria-involved apoptosis. *Toxicology Letters*. 201:92–100.

Powers, C.M., T.A. Slotkin, F.J. Seidler, A.R. Badireddy, and S. Padilla. 2011. Silver nanoparticles alter zebrafish development and larval behavior: Distinct roles for particle size, coating and composition. *Neurotoxicology and Teratology*. 33:708–714.

Powers, C.M., J. Yen, E.A. Linney, F.J. Seidler, and T.A. Slotkin. 2010. Silver exposure in developing zebrafish (Danio rerio): Persistent effects on larval behavior and survival. *Neurotoxicology and Teratology*. 32:391–397.

Rai, M.K., S.D. Deshmukh, A.P. Ingle, and A.K. Gade. 2012. Silver nanoparticles: the powerful nanoweapon against multidrug-resistant bacteria. *Journal of Applied Microbiology*. 112:841–852.

Rawson, D.M., T. Zhang, D. Kalicharan, and W.L. Jongebloed. 2000. Field emission scanning electron microscopy and transmission electron microscopy studies of the chorion, plasma membrane and syncytial layers of the gastrula-stage embryo of the zebrafish Brachydanio rerio: a consideration of the structural and functional relationships with respect to cryoprotectant penetration. *Aquaculture Research*. 31:325–336.

Roh, J., S.J. Sim, J. Yi, K. Park, K.H. Chung, D. Ryu, and J. Choi. 2009. Ecotoxicity of Silver Nanoparticles on the Soil Nematode Caenorhabditis elegans Using Functional Ecotoxicogenomics. *Environmental Science & Technology*. 43:3933–3940.

Römer, I., T.A. White, M. Baalousha, K. Chipman, M.R. Viant, and J.R. Lead. 2011. Aggregation and dispersion of silver nanoparticles in exposure media for aquatic toxicity tests. *Journal of Chromatography A*. 1218:4226–4233.

Shaw, B.J., and R.D. Handy. 2011. Physiological effects of nanoparticles on fish: A comparison of nanometals versus metal ions. *Environment International*. 37:1083–1097.

Skeaff, J., K. Delbeke, F. Van Assche, and B. Conard. 2000. A critical surface area concept for acute hazard classification of relatively insoluble metal-containing powders in aquatic environments. *Environmental toxicology and chemistry*. 19:1681–1691.

Skeaff, J.M., D.J. Hardy, and P. King. 2009. A new approach to the hazard classification of alloys based on transformation/dissolution. *Integrated environmental assessment and management*. 4:75–93.

Sotiriou, G.A., A. Teleki, A. Camenzind, F. Krumeich, A. Meyer, S. Panke, and S.E. Pratsinis. 2011. Nanosilver on nanostructured silica: Antibacterial activity and Ag surface area. *Chemical Engineering Journal*. 170:547–554.

Stensberg, M.C., Q. Wei, E.S. McLamore, D.M. Porterfield, A. Wei, and M.S. Sepúlveda. 2011. Toxicological studies on silver nanoparticles: challenges and opportunities in assessment, monitoring and imaging. *Nanomedicine*. 6:879–898.

Teeguarden, J.G., P.M. Hinderliter, G. Orr, B.D. Thrall, and J.G. Pounds. 2007. Particokinetics in vitro: dosimetry considerations for in vitro nanoparticle toxicity assessments. *Toxicological Sciences*. 95:300–312.

TRAP | Mid-Continent Ecology Division | US EPA.

Truong, L., S.L. Harper, and R.L. Tanguay. 2011. Evaluation of Embryotoxicity Using the Zebrafish Model. *In* Drug Safety Evaluation. J.-C. Gautier, editor. Humana Press, Totowa, NJ. 271–279.

Webster, T.J., D. Gorth, and D. Rand. 2011. Silver nanoparticle toxicity in Drosophila: size does matter. *International Journal of Nanomedicine*. 343.

Xia, T., Y. Zhao, T. Sager, S. George, S. Pokhrel, N. Li, D. Schoenfeld, H. Meng, S. Lin, X. Wang, M. Wang, Z. Ji, J.I. Zink, L. Mädler, V. Castranova, S. Lin, and A.E. Nel. 2011. Decreased Dissolution of ZnO by Iron Doping Yields Nanoparticles with Reduced Toxicity in the Rodent Lung and Zebrafish Embryos. *ACS Nano*. 5:1223–1235.

Yang, X., A.P. Gondikas, S.M. Marinakos, M. Auffan, J. Liu, H. Hsu-Kim, and J.N. Meyer. 2012. Mechanism of Silver Nanoparticle Toxicity Is Dependent on Dissolved Silver and Surface Coating in Caenorhabditis elegans. *Environmental Science & Technology*. 46:1119–1127.

Yeo, M., and M. Kang. 2008. Effects of nanometer sized silver materials on biological toxicity during zebrafish embryogenesis. *BULLETIN-KOREAN CHEMICAL SOCIETY*. 29:1179.

Zhang, W., Y. Yao, N. Sullivan, and Y. Chen. 2011. Modeling the Primary Size Effects of Citrate-Coated Silver Nanoparticles on Their Ion Release Kinetics. *Environmental Science & Technology*. 45:4422–4428.